J. Radiat. Res., 48, 219–231 (2007)

Regular Paper

Increased Chromosome Instability and Accumulation of DNA Double-strand Breaks in Werner Syndrome Cells

Kentaro ARIYOSHI[1,4], Keiji SUZUKI[2], Makoto GOTO[3], Masami WATANABE[1] and Seiji KODAMA[4]*

Chromosome Instability/DNA Double-strand Breaks/Werner Syndrome/Premature senescence/Oxidative stress/Genomic instability.

Werner syndrome (WS) is a premature aging syndrome caused by mutations of the *WRN* gene. Here, we demonstrate that a strain of WS fibroblast cells shows abnormal karyotypes characterized by several complex translocations and 50-fold more frequency of abnormal metaphases including dicentric chromosomes without fragments than normal cells when examined at a similar culture stage. Further, telomere fluorescence in situ hybridization indicates that the abnormal signals, extra telomere signal and loss of telomere signal, emerge two- to three-fold more frequently in WS cells than in normal cells. Taken together, these results indicate that chromosome instability including dysfunction of telomere maintenance is more prominent in WS cells than in normal cells. In addition, the accumulation of DNA double-strand breaks (DSBs) at the G_1 phase, including those at telomeres, detected by phosphorylated ATM (ataxia telangiectasia mutated) foci is accelerated in WS cells even at a low senescence level. The increased accumulation of DSBs in WS cells is reduced in the presence of anti-oxidative agents, suggesting that enhanced oxidative stress in WS cells is involved in accelerated accumulation of DSBs. These results indicate that WS cells are prone to accumulate DSBs spontaneously due to a defect of WRN, which leads to increased chromosome instability that could activate checkpoints, resulting in accelerated senescence.

INTRODUCTION

Werner syndrome (WS) is a rare recessive disorder, characterized by multiple progeroid features including graying and loss of hair, wrinkling of skin, cataracts, type II diabetes mellitus, osteoporosis, cardiovascular disease, and a high incidence of cancer.[1–3] Cells derived from WS patients exhibit shorter proliferative capacity,[4] an extended S phase,[5] and chromosomal instability referred to as variegated translocation mosaicism (VTM),[6,7] including clonal structural rearrangements associated with deletion-type mutation.[8,9] These features categorize WS as a chromosome instability syndrome.[10]

WS is caused by mutations of the *WRN* gene,[11] which encodes a protein (WRN) with activities of a 3' to 5' DNA helicase that belongs to the RecQ family and of a 3' to 5' exonuclease.[12] Hypersensitivity of WS cells to genotoxic reagents such as 4-nitroquinoline-1-oxide (4NQO)[9,13] and camptothecin,[14] and deficiency of correct recovery after replication arrest[15] suggest a role of WRN protein in DNA repair and replication. Recent studies concerning proteins that interact with WRN protein implicated WRN in DNA double-strand break (DSB) repair. WRN forms a complex with the Ku heterodimer[16–18] and serves as a substrate for DNA-dependent protein kinase catalytic subunit (DNA-PKcs).[19,20] In addition, it associates with RAD52[21] and co-localizes with RAD51 and replication protein A (RPA) after DNA damage.[22] Also, it interacts with MRE11 complex by binding to NBS1, of which function is defective in Nijmegen breakage syndrome (NBS).[23] These results suggest that insufficient repair ability for DSBs due to a defect of WRN may be causally related to premature senescent phenotypes in WS cells.

Recent studies demonstrate a close relationship between cellular senescence and accumulation of DSBs in the

*Corresponding author: Phone: +81-72-254-9855,
Fax: +81-72-254-9855,
E-mail: kodama@riast.osakafu-u.ac.jp
[1]Laboratory of Radiation Biology, Research Reactor Institute, Kyoto University, Osaka 590-0494, Japan; [2]Division of Radiation Biology, Department of Radiology and Radiation Biology, Graduate School of Biomedical Sciences, Nagasaki University, Nagasaki 852-8521, Japan; [3]Division of Anti-Ageing and Longevity Sciences, Faculty of Clinical Engineering, Toin University of Yokohama, Yokohama 225-8502, Japan; [4]Radiation Biology Laboratory, Radiation Research Center, Frontier Science Innovation Center, Organization for University-Industry-Government Cooperation, Osaka Prefecture University, Sakai, Osaka 599-8570, Japan.
doi:10.1269/jrr.07017

genome. For example, senescent normal human cells[24–26] and aged mice[26] accumulate nuclear foci of phosphorylated histone H2AX (γ-H2AX), suggesting that accumulation of DSBs contributes to the induction of cellular senescence. The location of γ-H2AX foci, however, is controversial; one report demonstrated that foci were co-localized with shortened telomeres[24] while another failed to find an association with telomeres.[26] Regardless of the location of the foci, these studies indicate that the DNA damage checkpoint response induced by DSBs may have a causal role in cellular senescence. While the reason for the accumulation of DSBs in senescent cells is not fully understood, it is noticed that senescent human fibroblast cells show reduced efficiency of non-homologous end joining (NHEJ) compared with young cells.[27] In addition, the fidelity of NHEJ is also compromised in pre-senescent and senescent cells,[27] resulting in the production of larger deletions at junctions. These results indicate that inefficient and aberrant joining may cause age-related genomic instability, which leads to a higher incidence of cancer in older generations.

In the present study, we studied the mechanism of accelerated senescence in WS cells in view of DNA damage induced by intracellular oxidative stress. Our results indicate that WS cells tend to accumulate DSBs, especially at the G_1 phase, probably due to defects in repairing DSBs and dealing with oxidative stress, leading to enhanced genomic instability represented as karyotype abnormalities including telomere dysfunction.

MATERIALS AND METHODS

Cells and cell culture

WS3RGB cells were fibroblasts obtained from a 42-year-old female Werner syndrome patient, and cultured in α-modified minimum essential medium (α-MEM; Invitrogen, CA, USA) supplemented with 10% fetal bovine serum (Trace Bioscience, Melbourne, Australia), 100 U/ml penicillin, and 100 μg/ml streptomycin. Normal human fibroblast cells, HE49,[28,29] were used as a control, and cultured in Eagle's minimal essential medium (MEM) supplemented with 10% fetal bovine serum, 100 U/ml penicillin, and 100 μg/ml streptomycin. Cells were maintained at 37°C in a humidified atmosphere with 5% CO_2. The growth rate (GR) was calculated using formula $GR = N_X/N_0$, where N_X is the number of cells per flask at subculture and N_0 is the number of cells inoculated into a flask.

Expression of the WRN protein

Western blot analysis for the WRN gene product was described previously.[9] Briefly, twenty μg of each protein extracted in radioimmunoprecipitation assay buffer were electrophoresed on a 7.5% SDS-polyacrilamide gel and then electrophoretically transferred to polyvinylidene difluoride membrane in transfer buffer (100 mM Tris and 192 mM glycine). The membrane was incubated at room temperature sequentially with blocking solution (10% skim milk) overnight, anti-WRN antibody (Santa Cruz biotechnology, Santa Cruz, CA) for 2 h, a biotinylated secondary antibody for 1h, and alkaline phosphatase streptavidine conjugate for 2 h. The band was visualized by incubation of the membrane for 2–3 min with a buffer [100 mM Tris, 100 mM NaCl, and 50 mM $MgCl_2$ (pH 9.5)] containing the substrate for alkaline phosphatase (nitroblue tetrazolium chloride and 5-bromo-4-chloro-3-indolyphosphate *p*- toluidine salt, Life Technologies, Inc.)

Senescence-associated-β-galactosidase (SA-β-gal) staining

Cells were rinsed once with Ca^{2+}- and Mg^{2+}- free phosphate-buffered saline (PBS (–)) and fixed with 2% paraformaldehyde solution containing 0.2% glutaraldehyde for 5 min at room temperature. After fixation, cells were rinsed extensively with PBS (–) and then incubated in SA-β-gal staining solution (40 mM citric acid/ sodium phosphate, pH 6.0, 5 mM potassium ferrocyanide, 5 mM potassium ferricyanide, 150 mM NaCl, 2 mM $MgCl_2$) containing 1 mg/ml 5-bromo-4-chloro-3-indolyl β-D-galactopyranoside (X-gal) which can stain senescent cells, as reported previously.[30]

Chromosome samples

Exponentially growing cells were treated with Colcemid (60 ng/ml) for 1.5 h, and harvested. Procedures for preparing chromosome samples and G-banding were described previously.[9]

Multi-color fluorescence in situ hybridization (FISH)

Multi-color FISH was performed according to the manufacturer's procedure (Cambio, Cambridge, UK). Briefly, a chromosome slide was aged on a hot plate at 65°C for 90 min, and denatured in solution (70% formamide in 2X SSC) at 65°C for 2 min. After quenching in ice-cold 70% ethanol for 4 min, the slide was dehydrated by serial washing for 5 min each in 70% ethanol and 100% ethanol, and dried at 37°C. An aliquot (10 μl) of probes for M-FISH was denatured at 65°C for 10 min and applied to the chromosome slide. The slide was covered with a glass coverslip and sealed with rubber cement to avoid evaporation. Hybridization was performed at 37°C for 48 h in a humidified atmosphere. After hybridization, the coverslip was removed, and the slide was washed twice for 5 min each in wash solution (50% formamide in 0.5X SSC) at 45°C, followed by incubating twice for 5 min each in 1X SSC at 45°C. The slide was then incubated for 4 min in detergent wash solution (0.05% detergent DT in 4X SSC) at 45°C. An aliquot (125 μl) of the detection reagent was applied to the slide, and the slide was covered with Parafilm, and then incubated in a humidified atmosphere for 20 min at 37°C. After removing the Parafilm, the slide was washed three times for 4 min each

in detergent wash solution at room temperature. Finally, DNA was couterstained with 4', 6-diamino-2-phenylindole (DAPI) in antifade solution. The chromosome images were captured and analyzed using the Leica CW4000 system.

Telomere-FISH analysis

Telomere-FISH analysis was performed by the procedure described previously.[31] For analysis of abnormal telomere signals induced by hydrogen peroxide at the G_2 phase of the cell cycle, exponentially growing cells were rinsed twice with PBS(–) and incubated with 200 μM hydrogen peroxide (H_2O_2) diluted in serum-free MEM for 1 h at 37°C. After treatment, cells were washed twice with complete MEM, incubated in complete MEM containing Colcemid (60 ng/ml) for 1.5 h, and harvested for preparation of chromosome samples.

Measurement of intracellular oxidative stress

Measurement of intracellular oxidative stress was based on the ability of cells to oxidize fluorogenic dyes to their corresponding fluorescent analogues. HE49 cells and WS3RGB cells cultured for three days and rinsed twice with PBS(–) followed by incubating in PBS(+) containing 5 μM 2',7'-dichlorodihydrofluorescein diacetate (H_2DCFDA) (Molecular Probes, OR, USA) for 30 min at 37°C. For the treatment with hydrogen peroxide (H_2O_2) or ascorbic acid (AsA), cells were rinsed twice with PBS(–), incubated at 37°C for 1 h in serum-free MEM containing 200 μM H_2O_2 or in complete MEM containing 200 μM AsA, and then further incubated in PBS(+) containing 5 μM H_2DCFDA for 30 min at 37°C. After dye incubation, cells were immediately harvested and subjected to fluorescence measurement using flow cytometry, where at least 15,000 cells were assayed in each condition. The fluorescence intensity of 2',7'-dichlorodihydrofluorescein was detected by FACScan (Beckton Dickinson Biosciences, NJ, USA)

Detection of DSBs at G_1, S, and G_2 phases by immunofluorescence assay

Detection of DSBs at G_1, S, and G_2 phases was performed according to the procedure described previously.[32] Cells grown on a coverslip to 60–70% confluence were washed once with cold cytoskelton (CSK) buffer, permeabilized with 0.5% Triton X-100 in CSK buffer for 5 min on ice, fixed with 4% paraformaldehyde in CSK buffer for 20 min, and immersed in 0.5% NP-40 in CSK buffer for 5 min at room temperature. The cells were then incubated for 2 h at 37°C with rabbit polyclonal anti-phosphorylated ataxia telangiectasia mutated (ATM) at Ser1981 antibody (Rockland, Philadelphia, PA, USA), and mouse monoclonal anti-phospho-histone H3 antibody (Upstate Biotechnology, New York, NY, USA), or mouse monoclonal anti-RPA (Calbiochem, La Jolla, CA, USA) at dilutions of 3:100, 1:100, and 1:100 in Tris-buffered saline (TBS), respectively. After washing with PBS(–) three times, the cells were incubated for 1 h at 37°C with Alexa Fluor 647-conjugated goat anti-rabbit antibody (Molecular Probes, Eugene, OR, USA) and Alexa Fluor 488-conjugated donkey anti-mouse antibody (Molecular Probes, Eugene, OR, USA) at each dilution of 1:1000 in TBS. Nuclei were counterstaind with DAPI (10 ng/ml in TBS) for 30 min, and coverslips were mounted on slide glasses with PBS(–) containing 10% glycerol. The samples were observed using a fluorescence microscope (Olympus, Tokyo) and digital images were recorded using a CCD camera (Olympus).

To identify the effect of anti-oxidative agents on the accumulation of DSBs, cells were incubated with 200 μM AsA or 1 mM ascorbic acid-2-glucoside diluted in complete MEM for 24 h at 37°C and then subjected to immunofluorescence.

Immuno-FISH assay for the detection of DSBs co-localized at telomeres

Immuno-FISH assay was performed as reported previously.[33] Briefly, cells were fixed, permeabilized, and stained with anti-phosphorylated ATM at Ser1981 antibody as described above. After staining, labeled protein was cross-linked with 4% paraformaldehyde in PBS(–) for 20 min at room temperature. The samples were then dehydrated in 70%, 85%, and 100% ethanol for 3 min each and air-dried. Then, DNA was denatured at 80°C for 30 min on a hotplate. After hybridization with a telomere-PNA probe for 5 h, cells were washed three times with 70% formamide/10 mM Tris (pH 6.8) for 15 min, followed by washing with PBS(–) for 5 min. Mounting and microscopic analysis were performed as described in the immunofluorescence assay.

RESULTS

Expression of the WRN protein

We first investigated the expression of WRN protein in normal human fibroblast cells (HE49) and WS fibroblast cells (WS3RGB) by Western blot analysis. As shown in Fig. 1, the WRN protein was expressed in HE49 cells. In contrast, no corresponding protein was found in WS3RGB cells, confirming that WS3RGB cells defects in the expression of WRN protein.

Spontaneous chromosome aberrations

To assess the senescence stage of HE49 cells and WS3RGB cells in culture, we cultured them by successive transfer until the growth rate (GR) was less than 1.0 per passage, with the result that the maximum population doubling numbers (PDN) of HE49 cells and WS3RGB cells were 59.5 and 33.2, respectively. As shown in Table 1, these cells showed a high percentage of SA-β-gal positive cells, *i.e.*, 74.9% for HE49 cells at PDN 52.5 and 69.5% for WS3RGB cells at PDN 29.3. Based on this observation, we referred to

the culture stage where a percentage of SA-β-gal positive cells was 70 or more as the pre-senescent stage.

To identify the role of WRN in chromosome stability, we analyzed spontaneous chromosome aberrations in WS3RGB cells at growing and pre-senescent stages and compared them with HE49 cells. As shown in Table 1, the appearance yield of the abnormal metaphase of WS3RGB cells at PDN 29.3 was 10.1%, which was almost 50-fold higher than that of HE49 cells (0.2%) at PDN 29.7 ($p < 0.01$, χ^2 test) when compared at similar culture stages. Similarly, abnormal metaphases appeared 3.7-fold more frequently in WS3RGB cells (10.1%) than in HE49 cells (2.7%) ($p < 0.05$, χ^2 test) when compared at similar senescent levels estimated by a percentage of SA-β-gal-positive cells, *i.e.*, 69.5% for WS3RGB and 74.9% for HE49. These results indicate that a defect of WRN promotes chromosomal instability, resulting in enhanced chromosomal abnormalities in WS cells.

Of particular interest is that all dicentric chromosomes observed in this study are not accompanied by fragments (Fig. 2A) because the appearance of this type of dicentric

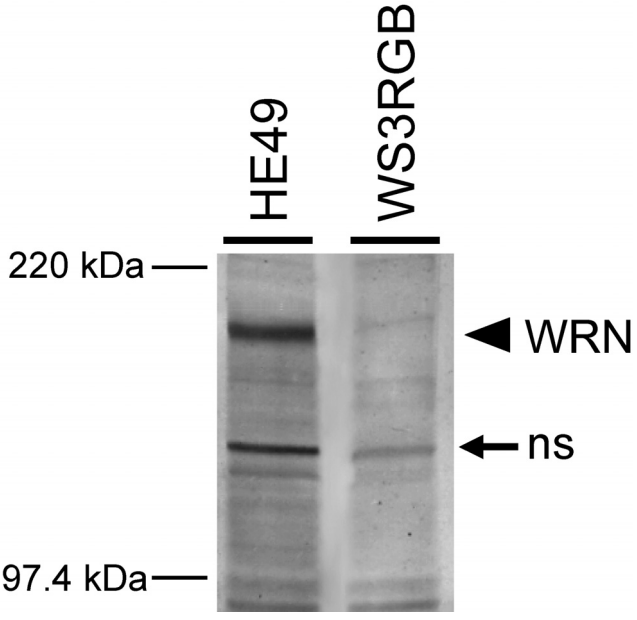

Fig. 1. Western blot analysis of the WRN protein. Twenty μg of total cell extracts were subjected to a SDS-PAGE, and the WRN proteins were detected anti-WRN antibody. HE49, normal human fibroblast cells; WS3RGB, fibroblast cells obtained from a Werner Syndrome patient; ns, stands for nonspecific.

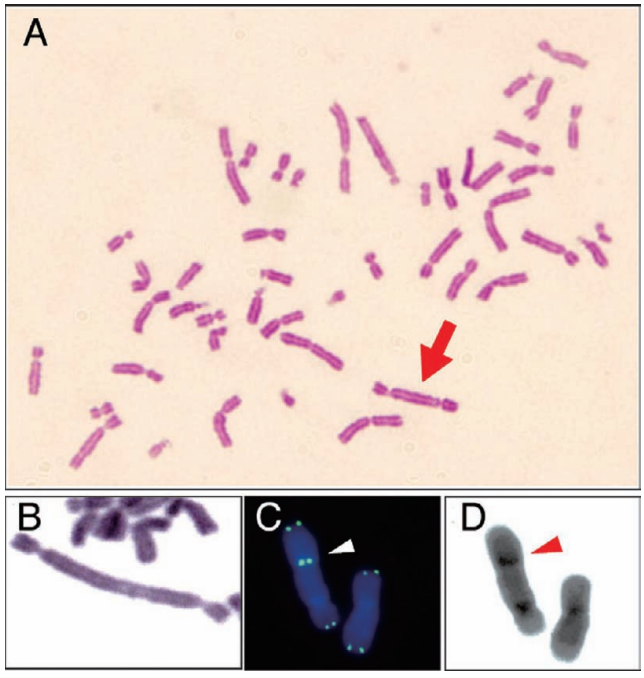

Fig. 2. Appearance of dicentric chromosomes that are not accompanied by fragments of WS3RGB cells during *in vitro* culture. (A) Metaphase spread showing a dicentric chromosome (arrow) without a fragment. (B) A representative dicentric chromosome presumed to be produced by sister union of a group B chromosome. (C) and (D) A dicentric chromosome stained with telomere FISH (C) or DAPI (D). Note that telomere signals were present at the fused position (arrowheads).

Table 1. Chromosome aberrations in HE49 cells and WS3RGB cells

Cell	Population doubling number	SA-β-gal -positive cells (%)[a]	No. of metaphases scored	No. of abnormal metaphases (%)		Gaps and breaks (%)		Dicentrics (%)	
HE49	29.7	2.3 ± 0.3	876	2 (0.2)	*	1 (0.1)	*	1 (0.1)	*
	31.2	3.3 ± 0.8	ND	ND		ND		ND	
	52.5	74.9 ± 5.4	74	2 (2.7)	*	1 (1.4)	*	1 (1.4)	*
WS3RGB	19.5	7.3 ± 1.7	ND	ND		ND		ND	
	26.0	28.8 ± 2.6	112	10 (8.9)	**	8 (7.2)	**	2 (1.8)	NS
	29.3	69.5 ± 3.1	287	29 (10.1)		26 (9.0)		3 (1.0)	

[a]Each value was calculated from three dishes and represented as mean ± S.D. *$p < 0.01$, χ^2 test, **$p < 0.05$, χ^2 test. NS, not significant. ND, not determined.

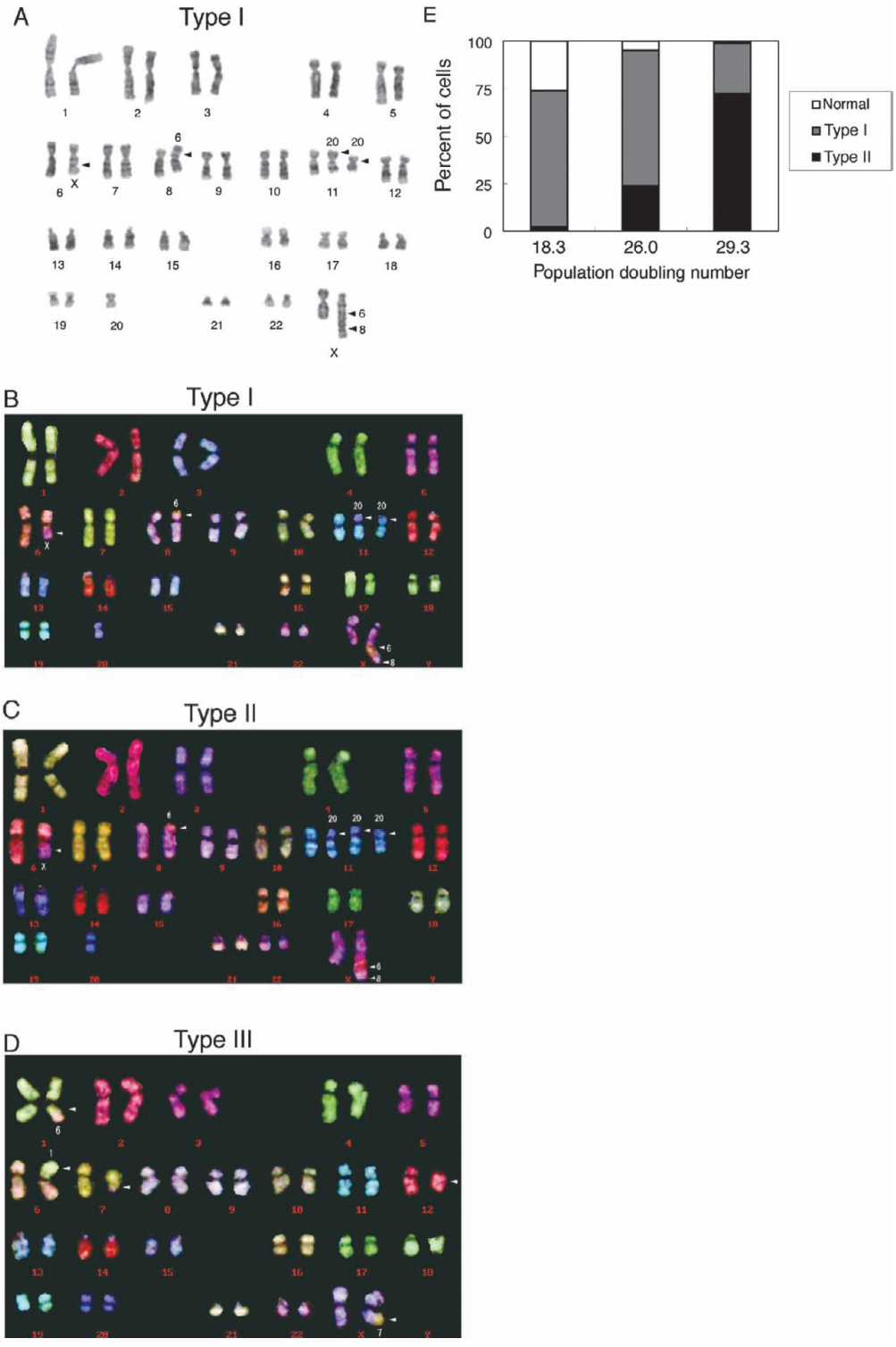

Fig. 3. Karyotype analysis of WS3RGB cells. (A) Type I karyotype of WS3RGB cells analyzed by G-banding. Note the presence of five translocations (see details below). Arrowheads represent break points of the translocations. (B)–(D) Karyotypes of WS3RGB cells analyzed by multi-color FISH; (B) Type I karyotype showing t(6p;8q), t(6q;Xp), t(6q;8p;Xq), t(11q;20q), and t(11p;20p), (C) Type II karyotype showing an extra t(11q;20q) in addition to type I, (D) Type III karyotype showing t(1q;6p), t(7q;Xq) and 12q-. (E) The increase in the subpopulation of cells possessing abnormal karyotypes in response to the population doubling number (PDN). At PDNs 18.3, 26.0, and 29.3, the percentage of cells having normal and abnormal karyotypes is determined. The number of cells analyzed was as follows: PDN 18.3, n = 129; PDN 26.0, n = 203; PDN 29.3, n = 105.

chromosome might be promoted by persistent deprotected telomeres.[33] As shown Table 1, WS3RGB cells showed 10-fold more frequency (1.0%) of spontaneous dicentric chromosomes without fragments than normal cells (0.1%) ($p < 0.01$, χ^2 test) when examined in culture at almost PDN 30. However, the frequency of dicentrics in HE49 cells and WS3RGB cells became similar, 1.4% and 1.0%, respectively, when examined at a similar senescence level estimated by a percentage of SA-β-gal-positive cells, *i.e.*, 74.9% for HE49 and 69.5% for WS3RGB. One dicentric chromosome observed in WS3RGB cells seemed to be produced by a sister union (Fig. 2B), the end-to-end fusion of sister chromatids. Evidence of telomere fusion in WS3RGB cells was partly confirmed by the presence of telomere signals at the

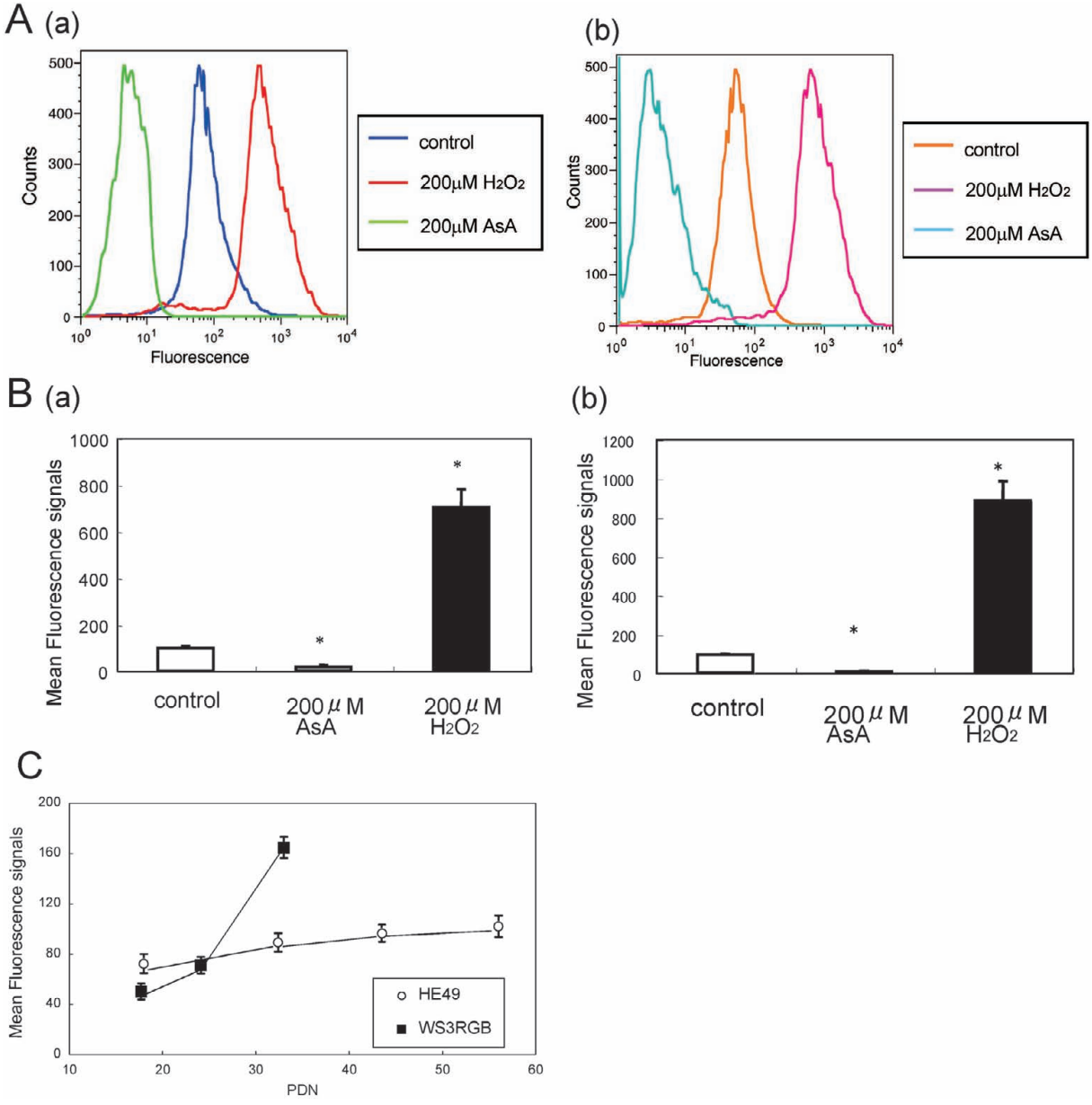

Fig. 4. Intracellular levels of oxidative stress. (A) Histograms represent the results of flow cytometry analysis for quantification of intracellular oxidative stress of HE49 cells (a) and WS3RGB cells (b) under untreated, H_2O_2-treated, and AsA-treated conditions. (B) The mean relative fluorescence units (RFU) of HE49 cells (a) and WS3RGB cells (b) under untreated, H_2O_2-treated, and AsA-treated conditions are calculated by flow cytometry analysis and represented. The data are calculated from three independent experiments and represented as mean ± S.E. The difference is significant by Student's t-test (*$p < 0.01$). (C) Changes of the RFU of HE49 cells and WS3RGB cells as a function of PDN in cell culture. The data are calculated from three independent experiments and represented as mean ± S.E.

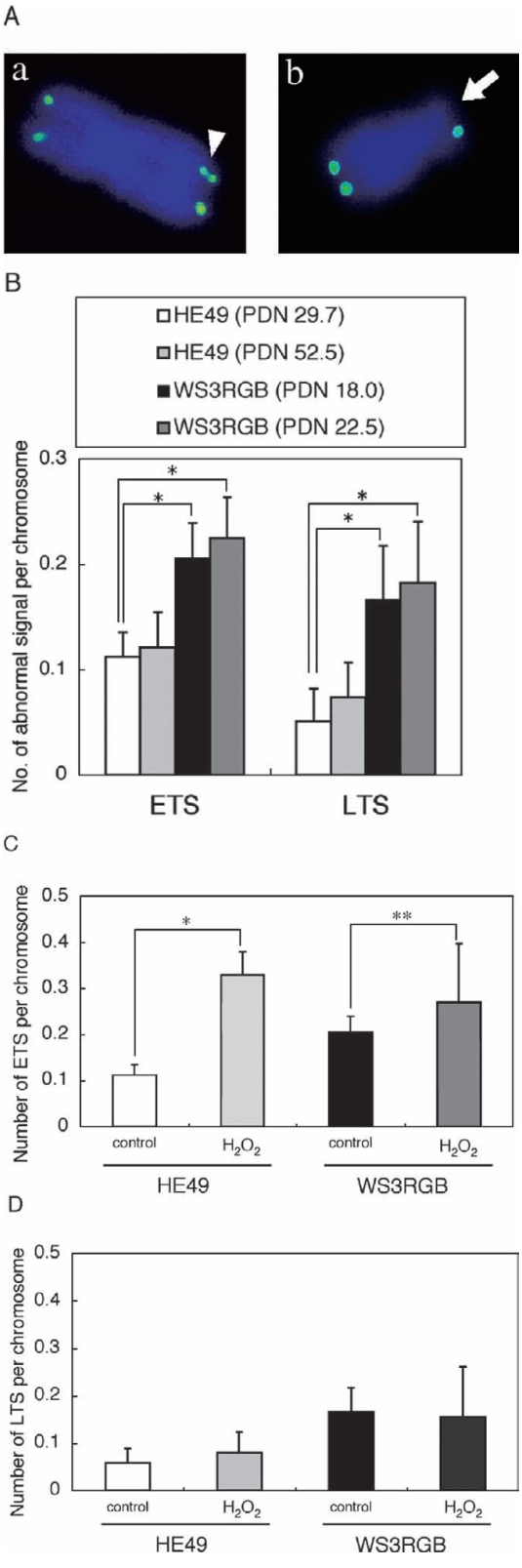

fused position of a dicentric chromosome detected by telomere fluorescence in situ hybridization (FISH) (Figs. 2C and 2D). Therefore, we suggest the possible involvement in telomere fusions in producing dicentrics without fragment.

Karyotype analysis of WS3RGB cells

As chromosomal abnormalities in WS cells were referred to as "variegated translocation mosaicism (VTM)", we investigated the karyotype of WS3RGB cells by G-banding and multi-FISH analyses. The result revealed that WS3RGB cells consisted of three different karyotypes such as types I-III. Among them, type I included five translocations such as t(6p;8q), t(6q;Xp), t(6q;8p;Xq), t(11q;20q), and t(11p;20p), as shown in Figs. 3A and 3B. Type II had an extra t(11q;20q) in addition to type I (Fig. 3C), and type III included t(1q;6p), t(7q;Xq), and 12q- (Fig. 3D). As shown in Fig. 3E, the majority (75%) of cells at PDN 18.3 showed abnormal karyotypes, *i.e.*, type I, and only 25% of cells possessed normal karyotypes. During culture passage *in vitro*, normal karyotype cells decreased gradually and disappeared in the pre-senescent stage at PDN 29.3. In contrast, cells possessing type II abnormal karyotypes increased and became dominant in the pre-senescent stage.

Intracellular levels of oxidative stress

To determine the level of intracellular oxidative stress, the ability of HE49 cells and WS3RGB cells to oxidize fluorogenic dyes to their corresponding fluorescent analogues was

Fig. 5. Telomere abnormalities detected by fluorescence in situ hybridization (FISH). (A) Representative telomere FISH photographs of an extra telomere signal (ETS) and loss of telomere signal (LTS). An arrowhead (a) and arrow (b) indicate ETS and LTS, respectively. (B) Abnormal telomere FISH signals at two different PDN levels in HE49 cells and WS3RGB cells. Number of cells analyzed is as follows: HE49 (PDN 29.7), n = 212; HE49 (PDN 52.5), n = 109; WS3RGB (PDN 18.0), n = 120; WS3RGB (PDN 22.5), n = 101. The differences are significant by Welch's t-test (*$p < 0.01$). (C) Induction of ETS by treatment with hydrogen peroxide (H_2O_2; 200 μM, 1h) in HE49 cells and WS3RGB cells. Cells were treated with hydrogen peroxide at the G_2 phase and the frequency of ETS was determined at the subsequent metaphase. The number of cells analyzed is as follows: HE49 (control), n = 212; HE49 (H_2O_2), n = 104; WS3RGB (control), n = 120; WS3RGB (H_2O_2), n = 68. The differences are significant by Welch's t-test (*$p < 0.01$, **$p < 0.05$). (D) Effect of treatment with hydrogen peroxide on LTS. Cells were treated with hydrogen peroxide at the G_2 phase and the frequency of LTS was determined at the subsequent metaphase. The number of cells analyzed is the same as those described in (C). No difference is observed between untreated control cells and H_2O_2-treated cells in both HE49 cells and WS3RGB cells. Abnormal telomere FISH signals are represented as $x/N \pm \sqrt{x/N}$, where x represented the number of abnormal signals and N represented the number of chromosomes scored.

measured using flow cytometry. Flow cytometry histograms shown in Fig. 4A represent the levels of intracellular oxidative stress of HE49 cells at PDN 26.0 and WS3RGB cells at PDN 24.1 under untreated, H_2O_2-treated, and AsA-treated conditions. The mean relative fluorescence units (RFU), calculated by FACScan, under untreated, H_2O_2-treated, and AsA-treated conditions were 96.2, 742, and 16.2, respectively, in HE49 cells (Fig. 4B-a), and 93.4, 886, 7.63, respectively, in WS3RGB cells (Fig. 4B-b). The result confirmed that 200 μM H_2O_2 treatment significantly enhanced the oxidative stress and, conversely, that 200 μM AsA treatment significantly decreased it. Essentially, there was no significant difference between HE49 cells and WS3RGB cells in terms of the levels of intracellular oxidative stress in response to the treatments with H_2O_2 and AsA (Figs. 4A-a and 4A-b). However, as shown in Fig. 4C, we found that the increase of the intracellular oxidative stress with increasing PDN was accelerated in WS3RGB cells compared with HE49 cells, suggesting that a defect of WRN was associated with the enhanced production of free radicals or the insufficient defense to free radicals.

Telomere abnormalities in WS3RGB cells

We postulated that telomere destabilization might be involved in the induction of dicentrics and abnormal karyotypes described above in WS3RGB cells. To examine this possibility, we investigated the presence of telomere sequences by telomere FISH analysis, and found two types of abnormal telomere signals such as an extra telomere signal (ETS) (Fig. 5A-a) and loss of telomere signal (LTS) (Fig. 5A-b). As shown in Fig. 5B, the frequencies of these abnormal telomere signals did not increase significantly with increasing PDN in both HE 49 cells and WS3RGB cells. However, these abnormal signals emerged two- to three-fold more frequently in

Table 2. Frequency of phosphorylated ATM foci with or without telomere FISH signals in HE49 cells and WS3RGB cells

Cell	Population doubling number	SA-β-gal -positive cells (%)[a]	No. of cells scored	No. of cells with pATM foci (%)	No. of cells with pATM foci with telomere signals (%)
HE49	31.2	3.3 ± 0.8	130	9 (6.9)	1 (0.8)
	52.5	74.9 ± 5.4	102	44 (43.1)	25 (24.5)
WS3RGB	19.5	7.3 ± 1.7	108	29 (26.8)	8 (7.4)
	26.0	28.8 ± 2.6	112	42 (37.5)	ND
	29.3	69.5 ± 3.1	100	38 (38.0)	14 (14.0)

[a]Each value was calculated from three dishes and represented as mean ± S.D. *$p < 0.01$, χ^2 test. NS, not significant. ND, not determined.

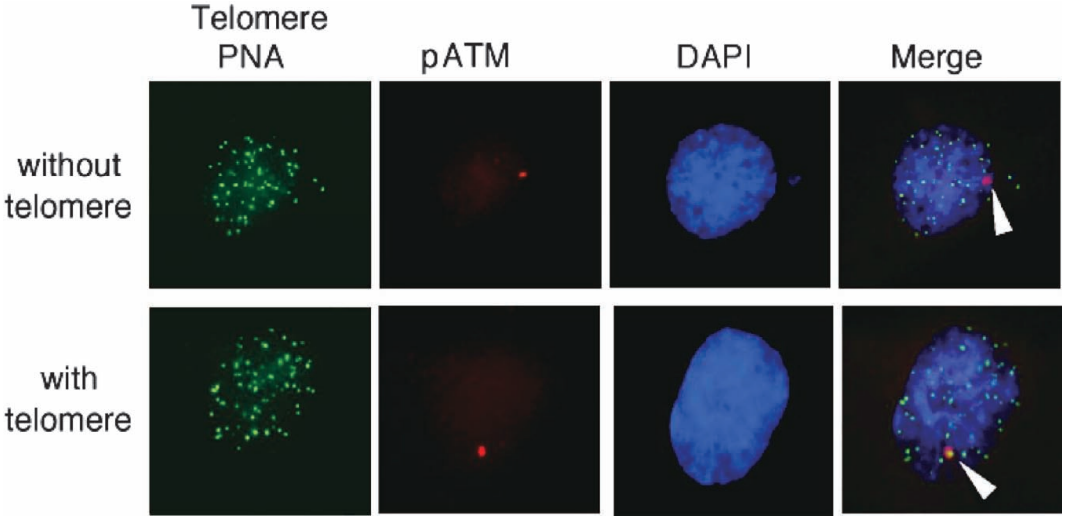

Fig. 6. Co-localization of DSBs at telomeres. DSBs visualized by phosphorylated ATM (pATM) foci and telomere FISH signals are concomitantly detected in HE49 cells and WS3RGB cells. Upper panels, pATM focus (arrowhead) is not co-localized with telomere signals in the nucleus of a WS3RGB cell; lower panels, pATM focus (arrowhead) is co-localized with a telomere signal in the nucleus of a WS3RGB cell.

WS3RGB cells than in HE49 cells (Fig. 5B), suggesting that WRN protein plays a role in telomere maintenance, the loss of which may cause unusual telomere structures expressed as ETS or LTS. Increased LTS in WS3RGB cells speculate that they have two- to three-fold higher incidence of relatively short telomeres than normal cells.

To identify the mechanisms for the appearance of ETS and LTS, we examined the effect of oxidative stress on the induction of these abnormal signals. Exposure to H_2O_2 (200 μM, 1 h) at the G_2 phase enhanced the induction of ETS at the subsequent metaphase in both HE49 cells and WS3RGB cells (Fig. 5C), suggesting that oxidative damage is involved in producing ETS. In contrast, LTS did not respond to treatment with hydrogen peroxide (Fig. 5D). These results suggest that reactive oxygen species (ROS) contribute to the production of ETS, but not LTS, if they exist at the G_2 phase in the cell cycle. It is very likely that LTS reflects the telomere status, which is not long enough to be detected by telomere FISH, suggesting that ROS emerging at the G_2 phase does not shorten telomeres. Although the molecular structures of ETS and LTS remain obscure, we speculate that dysfunction of telomere maintenance is responsible for the abnormal telomere signals observed in WS3RGB cells.

Accumulation of DSBs during cellular senescence

As treatment with H_2O_2 at the G_2 phase enhanced ETS frequency, we wondered whether DSBs were involved in the formation of ETS. To answer this question, we examined the spontaneous accumulation of DSBs in nuclei visualized by phosphorylated ATM (pATM) foci.[28,29,32] The number of pATM foci was not changed from almost one per cell in low to high senescent levels in culture when a percentage of SA-β-gal-positive cells was used as the senescence index (data not shown). In HE49 cells, the percentage of pATM-positive cells increased depending on the senescent level (Table 2), and was 43.1%, at the pre-senescent stage (SA-β-gal-positive cells, 74.9%), which was 6.2-fold higher than that (6.9%) at the young culture stage (SA-β-gal-positive cells, 3.3%) ($p < 0.01$, χ^2 test). The percentage of pATM-positive cells in WS3RGB cells (26.8%) was 3.9-fold more than that in HE49 cells (6.9%) at the young culture stage (SA-β-gal-positive cells, 7.3%) ($p < 0.01$, χ^2 test), and it increased to the maximum level (37.5%) at the middle culture stage (SA-β-gal-positive cells, 28.8%) ($p < 0.01$, χ^2 test) and remained the same level (38.0%) at the pre-senescent culture stage (SA-β-gal-positive cells, 69.5%) ($p < 0.01$, χ^2 test) (Table 2). These results indicate that cells retaining DSBs accumulate in a substantial population of the cell culture during cellular senescence and that this phenomenon, the accumulation of cells with DSBs, is accelerated in WS cells compared with normal cells.

Co-localization of DSB at telomeres

The percentage of cells showing co-localization of pATM foci on telomere signals was rare (0.8%) in HE49 cells at a young culture stage, but it was almost 9-fold higher (7.4%) in WS3RGB cells at a similar, young culture stage (Table 2 and Fig. 6) ($p < 0.01$, χ^2 test). This frequency increased according to progress in senescent levels in both cell strains; however, the enhancement ratio of cells showing co-localization of pATM foci on telomeres by progressive senescence was much higher in HE49 cells (30.6, 24.5/0.8) ($p < 0.01$, χ^2 test) than in WS3RGB cells (1.9, 14.0/7.4) (not significant, χ^2 test). In contrast to these results, as shown in Fig. 5B, ETS did not increase according to progress in senescent levels in both cell strains, suggesting that ETS was not a direct consequence of DSBs at telomeres.

Effect of anti-oxidative agents on the accumulation of DSBs

Since the accumulation of cells with DSBs was accelerated in WS cells compared with normal cells, we wondered how much oxidative stress contributes to this phenomenon. As shown in Fig. 7, ascorbic acid treatment (200 μM, 24 h) provided a 30% decrease of the percentage of pATM-positive cells in WS3RGB cells at PDN 26.0, while the same treatment gave rise to no change in HE49 cells at PDN 32.0 (Fig. 7) and at PDN 57.0 (data not shown). A similar result was obtained when cells were treated with ascorbic acid-2-glucoside (1 mM, 24 h; data not shown). These results suggest that oxidative stress contributes to accelerated accumulation of DSBs in a substantial population of WS3RGB cells.

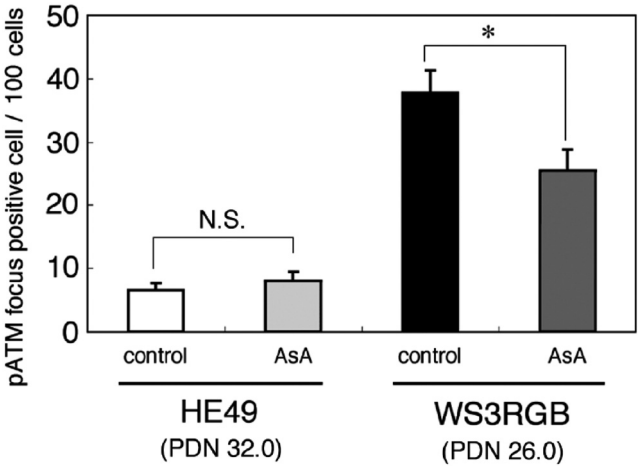

Fig. 7. Reduction of accumulation of DSBs by ascorbic acid (AsA) treatment in WS3RGB cells. Cells were incubated with 200 μM AsA for 24 h and then subjected to immunofluorescence for detection of pATM foci. Number of cells analyzed is as follows: HE49 (control), n = 300; HE49 (AsA), n = 200; WS3RGB (control), n = 201; WS3RGB (AsA), n = 200. The data are represented as mean ± S.D. The difference is significant by Student's t-test (*$p < 0.01$). N.S., not significant.

Accumulated DSBs in the G_1 phase

By combining immunofluorescence staining with antibodies against pATM and phospho-histone H3 or replication protein A, we distinguished the cell cycle phase of each cell as previously reported,[32] *i.e.*, S phase, replication protein A positive; G_2 phase, phospho-histone H3 positive; G_1 phase, negative for both markers, and measured the number of pATM positive cells in HE49 cells and WS3RGB cells at PDN levels 32.0 and 26.0, respectively. As shown in Fig. 8, at the G_1 phase, WS3RGB cells accumulated 6-fold more pATM positive cells compared with HE49 cells. At the G_2 phase, accumulation of pATM positive cells was almost 3-fold higher in WS3RGB cells than in HE49 cells. In contrast to G_1 and G_2 phases, no difference in the accumulation of pATM positive cells was observed in the S phase. These results indicate that WS cells accumulate DSBs at the G_1 phase preferentially although the accumulation of DSBs in normal cells is cell cycle-independent, suggesting the correlation with the increased senescence of WS3RGB cells compared with normal cells because of persistent DSBs.

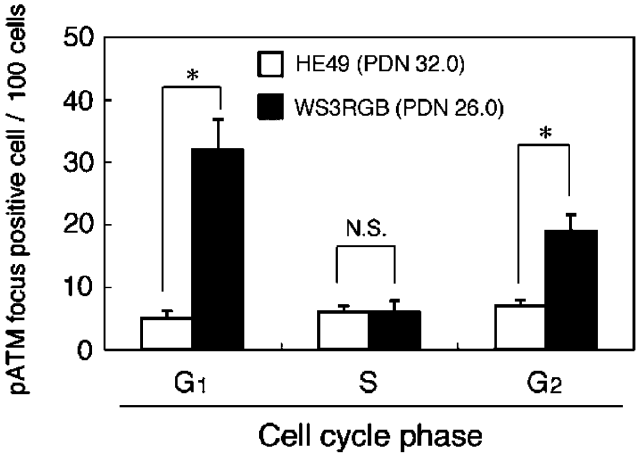

Fig. 8. Cell cycle-dependent accumulation of DSBs in WS3RGB cells but not in HE49 cells. Discrimination in cell-cycle phase of each cell is determined as follows: S phase, replication protein A positive; G_2 phase, phospho-histone H3 positive; G_1 phase, negative for both markers. Number of cells analyzed is as follows: G_1 phase, HE49, n = 100, WS3RGB, n = 100; S phase, HE49, n = 100, WS3RGB, n = 100; G_2 phase, HE49, n = 100, WS3RGB, n = 100. The data are represented as mean ± S.D. The differences are significant by Student's t-test (*$p < 0.01$). N.S., not significant.

DISCUSSION

In the present study, we demonstrated that the accumulation of DSBs, which preferentially occurs at the G_1 phase, is accelerated during cellular senescence of WS cells compared with normal cells. While the mechanism for the accumulation of excess DSBs in WS cells remains obscure, we speculate two possible reasons.

One is that WS cells have less ability than normal cells to deal with intracellular oxidative stress, which may accumulate more DNA damage in nuclei. We demonstrated that the increase of the intracellular oxidative stress with increasing PDN in cell culture was accelerated in WS cells compared with normal cells (Fig. 4C), suggesting an abnormal response to oxidative stress in WS cells. This possibility has been demonstrated in a substantial body of evidence. First, ascorbic acid, a typical anti-oxidative nutrient, delays cellular senescence more extensively in WS fibroblast cells than in normal fibroblast cells by reducing the rate of telomere shortening.[35] This suggests that lack of WRN renders telomeres more vulnerable to oxidative damage. Second, WS cells defect in poly ADP-ribosylation mediated by poly (ADP-ribose) polymerase-1 (PARP-1) after oxidative stress.[36] This diminution in protein modification leads to impairment of the base excision repair (BER) pathway, and this in turn increases cellular sensitivity to oxidative stress. Third, *in vivo* oxidative stress by ROS is elevated in both WS patients and mice with a mutation in the helicase domain of the mouse *WRN* gene,[37–39] suggesting that the defective function of WRN develops in the prooxidant state *in vivo*. These lines of evidence implicate a significant role of WRN protein in dealing with DNA damage caused by oxidative stress *in vitro* and *in vivo*.

Of particular interest is that WS cells accumulate DSBs in a cell cycle-dependent manner, showing a preferential accumulation of DSBs at the G_1 phase, meanwhile normal cells accumulate DSBs in a cell cycle-independent manner (Fig. 8). This finding is consistent with a recent report,[40] in which acute knockdown of WRN expression by RNA interference results in increased DNA damage detected by γ-H2AX foci in nonreplicating normal human fibroblast cells at the G_1 phase. Taken together, these results indicate that the formation of DSBs due to a lack of WRN function is not required for progression through the S phase. We speculate that G_1 checkpoint machinery prevents cells containing unrepairable DSB from progressing into the S phase, resulting in the accumulation of cells with DSBs at the G_1 phase. Similarly, G_2 checkpoint machinery may contribute to the substantial accumulation of cells at the G_2 phase in WS cells (Fig. 8); however, we cannot exclude the possibility that lack of WRN gives cells a differential sensitivity to the formation of DSBs at each cell-cycle phase.

The other possibility for the accumulation of excess DSBs in WS cells is that WS cells possess impaired repair capacity for DNA damage compared with normal cells. As mentioned already, WS cells are suggested to have increased ROS levels. Oxidative damage to DNA is known to induce a number of lesions, many of which include damage to single bases. Those lesions are mainly repaired by BER. The possibility of BER impairment in WS cells has been discussed above.

In addition, it is highly probable that DSBs are caused directly by oxidative stress or repair process of base damage by BER. The idea that WRN plays a role in processing DSBs is supported by evidence indicating its physical and functional interactions with proteins that have essential roles in two pathways of DSB repair, *i.e.*, non-homologous end joining (NHEJ) and homologous recombination (HR).[16–23] It is suggested that synergistic activity between WRN and Ku/DNA-PKcs is involved in the processing of broken DNA ends.[16–20] The role of WRN in NHEJ is further implicated by spectrum analyses of spontaneous mutations at the *HPRT* locus, which indicate that deletion-type mutations preferentially occur in WS cells.[8,9] A similar result is obtained by plasmid-based assays, where deletions at the rejoining point are much more extensive in WS cells than normal cells.[41] These results indicate that WRN functions in facilitating precise DSB repair and that lack of WRN results in the impairment of end joining in regard with efficiency and fidelity, suggesting that more irreparable DSB may remain in WS cells than in normal cells.

Recent studies have demonstrated that DSBs visualized by γ-H2AX foci accumulate during senescence of human cells in culture and in aging mice.[24–26] This indicates that during cellular senescence or organismal aging, mammalian cells accumulate persistent DNA lesions that include irreparable DSBs, supporting the idea that the accumulation of irreparable DSBs has a causal role in aging. Our result that the accumulation of DSBs is accelerated in WS cells in comparison to normal cells (Table 2) is in line with this idea, where the cause of cellular senescence emerges and accumulates at lower senescent levels in WS cells. Therefore, we propose that accelerated accumulation of DSBs contributes to the induction of premature senescence in WS cells.

Recently, a study that investigated the relationship between DSB repair and cellular senescence has revealed that the efficiency of end joining is reduced in pre-senescent and senescent cells, relative to young cells, and that end joining in old cells is associated with extended deletions,[27] indicating that DSB repair ability in senescent cells is less efficient and more error-prone compared with that in young cells. Intriguingly, the misrejoining characterized by extended deletions observed in senescent cells is consistent with a well-known WS phenotype as stated before.[8,9,41] Taken together, these findings speculate that the accumulation of DSBs observed in WS cells is a characteristic of senescent cells rather than a phenotype specific to WS cells. However, as shown in Table 2, the accumulation of DSBs is accelerated in WS cells compared with normal cells, which is possibly related to an abnormal WS phenotype, *i.e.*, short lifespan in culture.

Abnormal telomere dynamics due to a defect of WRN have been demonstrated in several studies.[42] For example, WS cells exhibit a faster rate of telomere erosion than normal cells although they senesce with longer telomeres than normal cells.[43] The expression of a dominant-negative, helicase-deficient WRN protein in normal cells causes stochastic loss of telomeric sequences and chromosome fusions.[44] In addition, lack of WRN helicase activity results in defective telomere lagging strand synthesis.[45] This is the first report to demonstrate that WS cells exhibit higher frequencies of abnormal telomere FISH signals, such as ETS and LTS, than normal cells (Fig. 5), and LTS might be responsible for the stochastic loss of telomere sequences, whereas molecular structure of ETS could not be defined. Regardless of the undefined nature of ETS, it is of interest that ETS is found in cells with characteristics of chromosome instability. They are cells from ataxia telangiectasia patients and $ATM^{-/-}$ mice,[46–48] lymphocytes from Fanconi anemia patients,[49] X-ray survived normal human fibroblast cells,[50] and embryonic stem cells of conditional TRF1 null mutant mice.[51] These lines of evidence suggest that the emergence of ETS is closely related to the induction of chromosomal instability. In fact, WS3RGB cells show a higher frequency of dicentric chromosomes possibly produced by end-to-end fusion (Fig. 2); however, because the average number of ETS per cell (10.0) is higher than that of DSBs per cell (1.0), DSBs are not responsible for the origin of ETS. The fact that the production of ETS is enhanced by hydrogen peroxide but reduced by anti-oxidative agents suggests that oxidative damage is involved in the induction of ETS; therefore, we speculate that ETS is a sensitive biomarker for oxidative stress and dysfunction of telomere maintenance.

It should be noticed that WS3RGB cells exhibit karyotype abnormality during successive transfer in cell culture (Fig. 3). WS3RGB cells containing type I karyotype preferentially increased in the near-senescent culture stage (PDN, 26.0), and cells containing type II karyotype became dominant by overcoming those with type I at the pre-senescent culture stage (PDN, 29.3)(Fig. 3E). As far as we know, primary human fibroblast cells derived from normal individuals never exhibit karyotype abnormality spontaneously during senescence in culture.[52] We speculate that dysfunction of telomere maintenance due to a defect in WRN may contribute to developing chromosome instability in WS3RGB cells.

In summary, the present study indicates that WS cells are prone to accumulate DSBs spontaneously due to a defect of WRN, which leads to increased chromosome instability that could activate checkpoints, resulting in accelerated senescence.

ACKNOWLEDGEMENTS

The authors thank M. Tsuji, Chromosome Science Labo Inc., for expert technical assistance with multi-color FISH analysis. This work was partly supported by a Grant-in Aid for Scientific Research from the Ministry of Education, Culture, Sports, Science and Technology of Japan.

REFERENCES

1. Salk, D. (1982) Werner's syndrome: a review of recent research with an analysis of connective tissue metabolism, growth control of cultured cells, and chromosomal aberrations. Hum. Genet. **62**: 1–5.
2. Goto, M., Miller, R. W., Ishikawa, Y. and Sugano, H. (1996) Excess of rare cancers in Werner syndrome (adult progeria). Cancer Epidemiol Biomarkers Prev. **5**: 239–246.
3. Martin, G. M., Oshima, J., Gray, M. D. and Poot, M. (1999) What geriatricians should know about the Werner syndrome. J. Am. Geriatr. Soc. **47**: 1136–1144.
4. Martin, G. M., Sprague, C. A. and Epstein, C. J. (1970) Replicative life-span of cultivated human cells. Effects of donor's age, tissue, and genotype. Lab. Invest. **23**: 86–92.
5. Takeuchi, F., Hanaoka, F., Goto, M., Yamada, M. and Miyamoto, T. (1982) Prolongation of S phase and whole cell cycle in Werner's syndrome fibroblasts. Exp. Gerontol. **17**: 473–480.
6. Hoehn, H., Bryant, E. M., Au, K., Norwood, T. H., Boman H. and Martin, G. M. (1975) Variegated translocation mosaicism in human skin fibroblast cultures. Cytogenet Cell Genet. **15**: 282–298.
7. Salk, D., Au, K., Hoehn, H. and Martin, G. M. (1981) Cytogenetics of Werner's syndrome cultured skin fibroblasts: variegated translocation mosaicism. Cytogenet Cell Genet. **30**: 92–107.
8. Fukuchi, K., Martin, G. M. and Monnat, R. J. Jr. (1989) Mutator phenotype of Werner syndrome is characterized by extensive deletions. Proc. Natl. Acad. Sci. USA **86**: 5893–5897.
9. Kodama, S., Kashino, G., Suzuki, K., Takatsuji, T., Okumura, Y., Oshimura, M., Watanabe, M. and Barrett, J. C. (1998) Failure to complement abnormal phenotypes of simian virus 40-transformed Werner syndrome cells by introduction of a normal human chromosome 8. Cancer Res. **58**: 5188–5195.
10. Meyn, M. S. (1997) Chromosome instability syndromes: lessons for carcinogenesis. Curr. Top. Microbiol. Immunol. **221**: 71–148.
11. Yu, C. E., Oshima, J., Fu, Y. H., Wijsman, E. M., Hisama, F., Alisch, R., Matthews, S., Nakura, J., Miki, T., Ouais, S., *et al.* (1996) Positional cloning of the Werner's syndrome gene. Science **272**: 258–262.
12. Huang, S., Li, B., Gray, M. D., Oshima, J., Mian, I. S. and Campisi, J. (1998) The premature ageing syndrome protein, WRN, is a 3'-->5' exonuclease. Nat. Genet. **20**: 114–116.
13. Poot, M., Gollahon, K. A., Emond, M. J., Silber, J. R. and Rabinovitch, P. S. (2002) Werner syndrome diploid fibroblasts are sensitive to 4-nitroquinoline-N-oxide and 8-methoxypsoralen: implications for the disease phenotype. FASEB J. **16**: 757–758.
14. Poot, M., Gollahon, K. A. and Rabinovitch, P. S. (1999) Werner syndrome lymphoblastoid cells are sensitive to camptothecin-induced apoptosis in S-phase. Hum. Genet. **104**: 10–14.
15. Pichierri, P., Franchitto, A., Mosesso, P. and Palitti, F. (2001) Werner's syndrome protein is required for correct recovery after replication arrest and DNA damage induced in S - phase of cell cycle. Mol. Biol. Cell **12**: 2412–2421.
16. Li, B. and Comai, L. (2000) Functional interaction between Ku and the Werner syndrome protein in DNA end processing. J. Biol. Chem. **275**: 28349–28352.
17. Orren, D. K., Machwe, A., Karmakar, P., Piotrowski, J., Cooper, M. P. and Bohr, V. A. (2001) A functional interaction of Ku with Werner exonuclease facilitates digestion of damaged DNA. Nucleic Acids Res. **29**:1926–1934.
18. Karmakar, P., Snowden, C. M., Ramsden, D. A. and Bohr, V. A. (2002) Ku heterodimer binds to both ends of the Werner protein and functional interaction occurs at the Werner N-terminus. Nucleic Acids Res. **30**: 3583–3591.
19. Yannone, S. M., Roy, S., Chan, D. W., Murphy, M. B., Huang, S., Campisi, J. and Chen, D. J. (2001) Werner syndrome protein is regulated and phosphorylated by DNA-dependent protein kinase. J. Biol. Chem. **276**: 38242–38248.
20. Karmakar, P., Piotrowski, J., Brosh, R. M. Jr, Sommers, J. A., Miller, S. P., Cheng, W. H., Snowden, C. M., Ramsden, D. A. and Bohr, V. A. (2002) Werner protein is a target of DNA-dependent protein kinase *in vivo* and *in vitro*, and its catalytic activities are regulated by phosphorylation. J. Biol. Chem. **277**: 18291–18302.
21. Baynton, K., Otterlei, M., Bjoras, M., Von Kobbe, C., Bohr, V.A. and Seeberg, E. (2003) WRN interacts physically and functionally with the recombination mediator protein RAD52. J. Biol. Chem. **278**: 36476–36486.
22. Sakamoto, S., Nishikawa, K., Heo, S. J., Goto, M., Furuichi, Y. and Shimamoto, A. (2001) Werner helicase relocates into nuclear foci in response to DNA damaging agents and co-localizes with RPA and Rad51. Genes Cells. **6**: 421–430.
23. Cheng, W. H., Von Kobbe, C., Opresko, P. L., Arthur, L. M., Komatsu, K., Seidman, M. M., Carney, J. P. and Bohr, V. A. (2004) Linkage between Werner syndrome protein and the Mre11 complex via Nbs1. J. Biol. Chem. **279**: 21169–21176.
24. d'Adda, di, Fagagna, F., Reaper, P. M., Clay-Farrace, L., Fiegler, H., Carr, P., Von Zglinicki, T., Saretzki, G., Carter, N. P. and Jackson, S. P. (2003) A DNA damage checkpoint response in telomere-initiated senescence. Nature **426**: 194–198.
25. Bakkenist, C. J., Drissi, R., Wu, J., Kastan, M. B. and Dome, J. S. (2004) Disappearance of the telomere dysfunction-induced stress response in fully senescent cells. Cancer Res. **64**: 3748–3752.
26. Sedelnikova, O. A., Horikawa, I., Zimonjic, D. B., Popescu, N. C., Bonner, W. M. and Barrett, J. C. (2004) Senescing human cells and ageing mice accumulate DNA lesions with unrepairable double-strand breaks. Nat. Cell Biol. **6**: 168–170.
27. Seluanov, A., Mittelman, D., Pereira-Smith, O. M., Wilson, J. H. and Gorbunova, V. (2004) DNA end joining becomes less efficient and more error-prone during cellular senescence. Proc. Natl. Acad. Sci. USA **101**: 7624–7629.
28. Suzuki, M., Suzuki, K., Kodama, S. and Watanabe, M. (2006) Interstitial chromatin alteration causes persistent p53 activation involved in the radiation-induced senescence-like growth arrest. Biochem. Biophys. Res. Commun. **340**: 145–150.
29. Suzuki, M., Suzuki, K., Kodama, S. and Watanabe, M. (2006) Phosphorylated histone H2AX foci persist on rejoined mitotic chromosomes in normal human diploid cells exposed to ion-

izing radiation. Radiat. Res. **165**: 269–276.
30. Dimri, G. P., Lee, X., Basile, G., Acosta, M., Scott, G., Roskelley, C., Medrano, E. E., Linskens, M., Rubelj, I., Pereira-Smith, O., *et al*. (1995) A biomarker that identifies senescent human cells in culture and in aging skin *in vivo*. Proc. Natl. Acad. Sci. USA **92**: 9363 – 9367.
31. Urushibara, A., Kodama, S., Suzuki, K., Desa, M. B., Suzuki, F., Tsutsui, T. and Watanabe, M. (2004) Involvement of telomere dysfunction in the induction of genomic instability by radiation in scid mouse cells. Biochem. Biophys. Res. Commun. **313**: 1037–1043.
32. Suzuki, K., Okada, H., Yamauchi, M., Oka, Y., Kodama, S. and Watanabe, M. (2006) Qualitative and quantitative analysis of phosphorylated ATM foci induced by low-dose ionizing radiation. Radiat. Res. **165**: 499–504.
33. Herbig, U., Jobling, W. A., Chen, B. P., Chen, D. J. and Sedivy, J. M. (2004) Telomere shortening triggers senescence of human cells through a pathway involving ATM, p53, and $p21^{CIP1}$, but not $p16^{INK4a}$. Mol. Cell **14**: 501–513.
34. Celli, G. B. and de Lange, T. (2005) DNA processing is not required for ATM-mediated telomere damage response after TRF2 deletion. Nat. Cell Biol. **7**: 712–718.
35. Kashino, G., Kodama, S., Nakayama, Y., Suzuki, K., Fukase, K., Goto and M., Watanabe, M. (2003) Relief of oxidative stress by ascorbic acid delays cellular senescence of normal human and Werner syndrome fibroblast cells. Free Radic. Biol. Med. **35**: 438–443.
36. Von Kobbe, C., Harrigan, J. A., May, A., Opresko, P. L., Dawut, L., Cheng, W. H. and Bohr, V. A. (2003) Central role for the Werner syndrome protein/poly (ADP-ribose) polymerase 1 complex in the poly (ADP-ribosyl)ation pathway after DNA damage. Mol. Cell Biol. **23**: 8601–8613.
37. Pagano, G., Zatterale, A., Degan, P., d'Ischia, M., Kelly, F. J., Pallardo, F. V. and Kodama, S. (2005) Multiple involvement of oxidative stress in Werner syndrome phenotype. Biogerontology. **6**: 233–243.
38. Pagano, G., Zatterale, A., Degan, P., d'Ischia, M., Kelly, F. J., Pallardo, F. V., Calzone, R., Castello, G., Dunster, C., Giudice, A., *et al*. (2005) *In vivo* prooxidant state in Werner syndrome (WS): results from three WS patients and two WS heterozygotes. Free Radic. Res. **39**: 529–533.
39. Massip, L., Garand, C., Turaga, R. V., Deschenes, F., Thorin, E. and Lebel, M. (2005) Increased insulin, triglycerides, reactive oxygen species, and cardiac fibrosis in mice with a mutation in the helicase domain of the Werner syndrome gene homologue. Exp Gerontol. **41**: 157–168.
40. Szekely, A. M., Bleichert, F., Numann, A., Van Komen, S., Manasanch, E., Ben Nasr, A., Canaan, A. and Weissman, S. M. (2005) Werner protein protects nonproliferating cells from oxidative DNA damage. Mol. Cell Biol. **25**: 10492–10506.
41. Oshima, J., Huang, S., Pae, C., Campisi, J. and Schiestl, R. H. (2002) Lack of WRN results in extensive deletion at nonhomologous joining ends. Cancer Res. **62**: 547–551.
42. Orren, D. K. (2006) Werner syndrome: molecular insights into the relationships between defective DNA metabolism, genomic instability, cancer and aging. Front Biosci. **11**: 2657–2671.
43. Schulz, V. P., Zakian, V. A., Ogburn, C. E., McKay, J., Jarzebowicz, A. A., Edland, S. D. and Martin, G. M. (1996) Accelerated loss of telomeric repeats may not explain accelerated replicative decline of Werner syndrome cells. Hum Genet. **97**: 750–754.
44. Bai, Y. and Murnane, J. P. (2003) Telomere instability in a human tumor cell line expressing a dominant-negative WRN protein. Hum Genet. **113**: 337–347.
45. Crabbe, L., Verdun, R. E., Haggblom, C. I. and Karlseder, J. (2004) Defective telomere lagging strand synthesis in cells lacking WRN helicase activity. Science **306**: 1951–1953.
46. Hande, M. P., Balajee, A. S., Tchirkov, A., Wynshaw-Boris, A. and Lansdorp, P. M. (2001) Extra-chromosomal telomeric DNA in cells from Atm(–/–) mice and patients with ataxia-telangiectasia. Hum. Mol. Genet. **10**: 519–528.
47. Tchirkov, A. and Lansdorp, P. M.(2003) Role of oxidative stress in telomere shortening in cultured fibroblasts from normal individuals and patients with ataxia-telangiectasia. Hum. Mol. Genet. **12**: 227–232.
48. Undarmaa, B., Kodama, S., Suzuki, K., Niwa, O. and Watanabe, M. (2004) X-ray-induced telomeric instability in Atm-deficient mouse cells. Biochem. Biophys. Res. Commun. **315**: 51–58.
49. Callen, E., Samper, E., Ramirez, M. J., Creus, A., Marcos, R., Ortega, J. J., Olive, T., Badell, I., Blasco, M. A. and Surralles, J. (2002) Breaks at telomeres and TRF2-independent end fusions in Fanconi anemia. Hum. Mol. Genet. **11**: 439–444.
50. Ojima, M., Hamano, H., Suzuki, M., Suzuki, K., Kodama S. and Watanabe, M. (2004) Delayed induction of telomere instability in normal human fibroblast cells by ionizing radiation. J. Radiat. Res. **45**: 105–110.
51. Iwano, T., Tachibana, M., Reth, M. and Shinkai, Y. (2004) Importance of TRF1 for functional telomere structure. J. Biol. Chem. **279**: 1442–448.
52. Romanov, S. R., Kozakiewicz, B. K., Holst, C. R., Stampfer, M. R., Haupt, L. M. and Tlsty, T. D. (2001) Normal human mammary epithelial cells spontaneously escape senescence and acquire genomic changes. Nature **409**: 633–637.

Received on February 21, 2007
Revision received on March 13, 2007
Accepted on March 13, 2007
J-STAGE Advance Publication Date: April 23, 2007